Journal Pre-proof

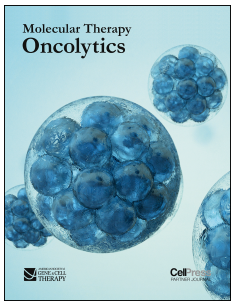

Toward comprehensive imaging of oncolytic viroimmunotherapy

Shyambabu Chaurasiya, Sang-In Kim, Michael O'Leary, Anthony K. Park, Jianming Lu, Seonah Kang, Zhifang Zhang, Annie Yang, Yanghee Woo, Yuman Fong, Susanne G. Warner

PII: S2372-7705(21)00090-5

DOI: https://doi.org/10.1016/j.omto.2021.06.010

Reference: OMTO 424

To appear in: *Molecular Therapy: Oncolytics*

Please cite this article as: Chaurasiya S, Kim S-I, O'Leary M, Park AK, Lu J, Kang S, Zhang Z, Yang A, Woo Y, Fong Y, Warner SG, Toward comprehensive imaging of oncolytic viroimmunotherapy, *Molecular Therapy: Oncolytics* (2021), doi: https://doi.org/10.1016/j.omto.2021.06.010.

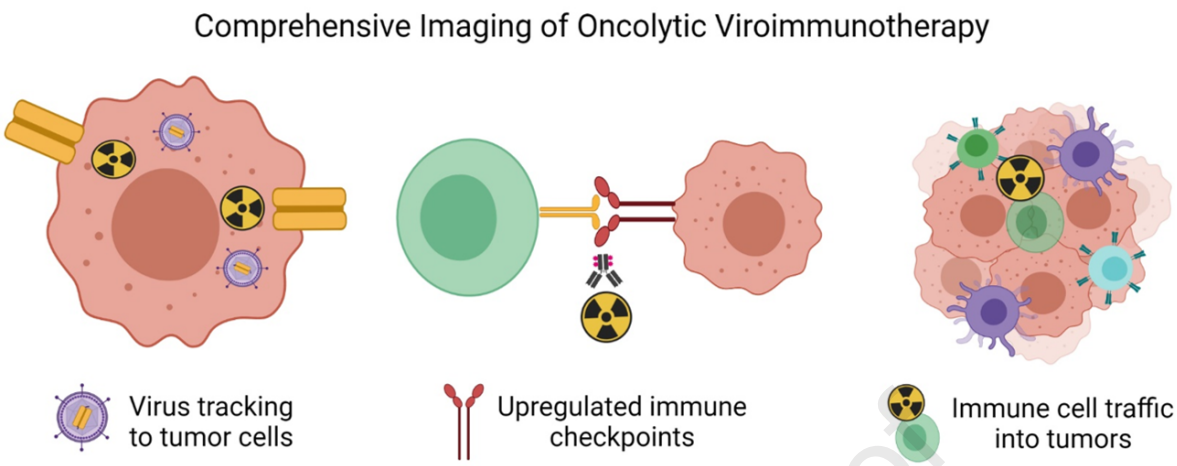

Title: Toward comprehensive imaging of oncolytic viroimmunotherapy

Authors: Shyambabu Chaurasiya[1*], Sang-In Kim[1*], Michael O'Leary[1], Anthony K. Park[2], Jianming Lu[1], Seonah Kang[1], Zhifang Zhang[1], Annie Yang[1], Yanghee Woo[1], Yuman Fong[1], Susanne G. Warner[1]

[1]Department of Surgery, Division of Surgical Oncology, City of Hope National Medical Center, Duarte, CA 91010, USA

[2]Center for Gene Therapy, Department of Hematologic and Hematopoietic Cell Transplantation, Beckman Research Institute, City of Hope National Medical Center, Duarte, CA 91010, USA

*These authors contributed equally

Correspondence should be addressed to:

Susanne Warner MD

1500 E. Duarte Rd.

Pavilion 2226

Duarte, CA 91010

USA

Email: suwarner@coh.org

Phone: 626-218-0060

Fax: 626-471-6212

Short title: Optical and functional imaging of CF33-platform

ABSTRACT

Oncolytic viruses infect, replicate in, and kill cancer cells, leaving normal cells unharmed; they also recruit and activate immune cells against tumor cells. While clinical indications for viroimmunotherapy are growing, barriers to widespread treatment remain. Ensuring real-time tracking of viral replication and resulting anti-tumor immune responses will overcome some of these barriers and is thus a top priority. Clinically optimizing trackability of viral replication will promote safe dose increases, guide serial dosing, and enhance treatment effects. However, viral delivery is only half the story. Oncolytic viruses are known to upregulate immune checkpoint expression thereby priming otherwise immunodeficient tumor immune microenvironments for treatment with checkpoint inhibitors. Novel modalities to track virus-induced changes in tumor microenvironments include non-invasive measurements of immune cell populations and responses to viroimmunotherapy such as: 1) In situ use of radiotracers to track checkpoint protein expression or immune cell traffic, and 2) Ex vivo labelling of immune cells followed by nuclear medicine imaging. Herein, we review clinical progress toward accurate imaging of oncolytic virus replication, and further review current status of functional imaging of immune responses to viroimmunotherapy.

KEYWORDS: Oncolytic viral therapy, theranostic imaging, viroimmunotherapy

INTRODUCTION

Oncolytic viruses (OVs) are a powerful tool of immunogenicity and are capable of conferring anti-tumor immunity even to disseminated cancers. While one virus is currently FDA-approved for melanoma treatment, barriers remain to the widespread use of viroimmunotherapy in solid tumor treatment algorithms. With an average time to response of approximately 4 months as seen in the OPTIM trial prompting talimogene laherparepvec (T-Vec) approval,[1-3] oncolytic virologists and medical oncologists alike are left to guess whether or not continued OV or other cancer treatment dosing will benefit the patient. This is especially harrowing in the setting of pseudo-progression or progression prior to response, which can occur in up to 49% of responders.[4,5] In many cases, we simply continue to treat until a tumor marker rises, or an image demonstrates definitive tumor progression, unaware if we have benefited the patient with the preceding months of therapy. The inability to non-invasively measure treatment progress in real-time is a barrier shared by OVs, immunotherapies, and traditional cytotoxic treatments alike. Non-invasive diagnostics that can provide valid feedback would save money, time, and toxicity for many.

Attempts at optimizing clinical imaging of viral replication in tumors have been ongoing over the last 20 years with limited success.[6] Real-time imaging allows OVs to meet their full theranostic potential. Indeed, many OVs currently in clinical testing accommodate transgenes encoding "payloads" that include enhancement of immunogenicity and also reporter genes that allow for real-time tracking of viral replication. Given that many OVs are tumor-tropic, viral imaging may elucidate previously undetected tumors. Ultimately, imaging of OV trafficking and viability could yield truly personalized medicine by guiding variables like future serial injections for

intratumoral models and dose increases for systemic delivery. However, despite years of clinical development spanning disease and vector types, optimal dose timing and the best vector and dosing strategy for each specific tumor remains a challenge.[7]

Thus far, there are two predominant types of real-time OV imaging: optical and deep tissue functional imaging. Clinically, optical imaging allows direct visualization of fluorescence. In the operating room, special laparoscopes can elucidate fluorescent tissue within body cavities; In the clinic, lamps can reveal fluorescent epidermal or mucosal surfaces.[8] Functional viral imaging measures isotope uptake as a surrogate for viral replication with scans like positron emission tomography (PET) or single photon emission computed tomography (SPECT). Of the reporter-genes in OV clinical trials, human sodium iodide symporter (hNIS) is the most prominent.[9] However, only a select few investigators have published actual human images.[8,10-15]

While critical to the success of the field, tracking viral delivery is only half the story. Reliable non-invasive characterization of virally-induced anti-tumor immune responses also remains elusive. In vivo and ex vivo techniques for radiolabeling immune cells, cytokines, and co-stimulators or co-inhibitors are rapidly evolving arenas of clinical imaging. To most comprehensively understand the anti-tumor effects of viroimmunotherapy without invasively sampling tissue, non-invasive imaging should include viral tracking, measurement of immune checkpoint expression, and tracking immune cells into tumors. Herein, we review progress and promise of comprehensive non-invasive imaging of viroimmunotherapy.

Review of published clinical real-time viral tracking

As demonstrated by our group and others, real-time tracking of viral replication demonstrates tumor tropism whether viruses are administered intratumorally (IT), intravenously (IV), or intraperitoneally (IP) (**Figure 1)**.[16,17] These experiments were confirmed in previously published experiments using HCT116 xenografts,[17] and also as shown here using HT-29 xenografts infected with a recombinant orthopoxvirus platform (CF33) with *tk* deletion encoding either human sodium iodine symporter (CF33-hNIS) or firefly luciferase (CF33-Luc).[16,17]

Upon comprehensive English literature review from 1995 to present, many abstracts and posters referencing images on replicating oncolytic viruses were found. However, a surprising paucity of peer-reviewed publications showed images of non-invasive viral replication tracking. The authors were only able to identify six peer-reviewed publications with images of viral replication: four studies demonstrated successful tracking of NIS-encoding OVs via I-123 SPECT/CT, one study used ^{18}F-labeled penciclovir analogue, and one used the ^{124}I-labeled substrate for HSV-1-*tk* to monitor thymidine kinase gene expression **(Table 1)**. In each of the described studies, the success of imaging appeared dose-dependent. In the NIS-based studies, images appeared most consistently 7-8 days after treatment.[10-12] In the *tk* imaging papers, Jacobs et al. show [^{124}I]-FIAU retention 68 hours after injection whereas Penuelas et al. examined [^{18}F]-FHBG signal 1 week post-injection.[14,15] In the remaining trial referenced in Table 1, investigators of a GFP-encoding vaccinia used fluorescent lamps in clinic to examine pox-like rash occurring in treated patients with head and neck carcinomas. While this does not represent imaging of viral replication in tumors, the investigators emphasize that such a rash confirms successful systemic viral replication.[8]

Clinical OV image optimization has remained a challenge despite numerous creative adjuncts like oral contrast,[18] chemo-tagged radiotracers, and novel highly-specific tracers.[19] Moreover, in addition to the expected variability of viral replication between tumor types, even similar types of tumors in identical anatomic locations exhibit differing can vary. For instance, Rajecki et al treated a cervical cancer patient with Ad5/3-Δ24-hNIS, acting based upon the findings of Barton et al. using Ad5-yCD/*mut*TK_{SR39}*rep*-hNIS in prostate cancer.[13,20] Unfortunately, Rajecki and colleagues saw no evidence of OV-based signal. This may have been due to their study of both a different vector with hNIS on a different promoter, and also an entirely different disease type. Groups using hNIS-based imaging have seen more consistent results at higher doses and with more uniform disease states as detailed in **Table 1**. However, published images demonstrate that further optimization is needed to achieve clinical relevance. Perhaps clinical optimization using a more potent and rapidly replicating virus platforms like CF33 or herpes simplex viruses encoding hNIS will render consistent high-yield imaging to guide future therapies. If properly established, real-time non-invasive deep tissue imaging will enable more rapid incorporation of imageable viroimmunotherapies into solid tumor treatment schema.

Viral replication co-localizes with tumor T cell infiltration

To further assess whether non-invasive viral imaging can serve as a linear surrogate for both viral replication and T cell infiltration, we confirmed that immunofluorescent vaccinia staining corresponds to immunohistochemical (IHC) staining showing T cells co-localizing with viral infection **(Figure 2A&B)**. Moreover, in subsequent experiments, we evaluated immune cell infiltration and confirmed these IHC findings quantitatively using FACS of tumor lysates to find that CD8+ tumor infiltration is higher in viral-treated tumors **(Figure 2C)**. We and others have

shown that CD8+ T cells co-localize to actively replicating virus.[21] This is aligned with findings by Sampath et al. which showing direct synergistic interactions between an enveloped vaccinia virus and immune cell components.[22] While co-localized viral particles and immune cells suggest that non-invasive imaging of viral replication corresponds to immune cell trafficking, only by specifically imaging immune cells or invasively sampling tumors can we confirm this.

Imaging virally-induced immune checkpoint expression

Our group and others have demonstrated upregulated PD-L1 in tumors following poxvirus infection.[23,24] Many feel such upregulation mediates the success of combination therapies pairing oncolytic viruses with checkpoint inhibitors in advanced solid tumors.[25] Others feel that viruses pair well with checkpoint inhibitors simply because they release inflammatory damage- and pathogen-associated proteins into the tumor microenvironment, thereby recruiting and activating immune cells in the tumor microenvironment.[26] In order to find the most effective place in treatment algorithms for oncolytic viruses amid the already tumultuous sea of immune checkpoint inhibitors available, we must fully characterize both checkpoint expression and immune cell trafficking in real time. While reliably imaging checkpoint expression after immunotherapy treatment of any sort is a tall order, there is some progress with radiolabeled antibodies to a variety of checkpoint proteins **(Figure 3)**. Indeed, one can image any point along the continuum of activating a T cell as it recognizes tumor, from radio-labeled antibodies to cytokines like IFNγ, cluster of differentiation (CD) cell-surface proteins like CD8, or markers of activation like granzyme B. At present, in vivo imaging of this nature is plagued by non-specific background uptake. That said, some progress is being made with highly specific radiotracers and anti-bodies.[27]

Current clinical progress in tracking immune responses to oncolytic virus

To date, imaging of immune responses to viral therapy are sparsely explored. Weibel et al. in 2013 correlated ^{19}F-Magnetic Resonance Imaging (MRI) with CD68 staining on IHC in xenograft models of human melanoma and breast cancer infected with an oncolytic vaccinia virus GLV-1h68.[28] These macrophage-dense regions within a tumor tended to surround virally infected areas of tumor as confirmed with immune-fluorescent staining. While this suggests that ^{19}F-MRI could serve as a surrogate for tracking immune response to treatment, clinical translatability of these findings in nude mice is questionable. To take the next steps as a field in imaging immune responses to oncolytic viral therapy, we will need to draw from the experiences of our adoptive immune cell colleagues.

Ex vivo radiolabeling of T cells holds promise to help track efficacy of immunotherapies **(Figure 4)** in terms of immune cell recruitment.[29] While this is most broadly explored to track T cells bearing radiolabeled chimeric antigen receptors, simple co-culture of T cells with radioisotope is also an effective means of tracking tumor infiltration. Perhaps the most clinically advanced form of in vivo targeting and also adoptive cell radiolabeling is found in Zirconium (89-Zr).[30] Notably more specific than other tracers such as 18-F given its independence from glucose metabolism,[31] 89-Zr also has the advantages of a long half-life (3.3 days) making it helpful for tracking cells over at least several days with serial CT-PET imaging.[30] Moreover, its relatively lower positron energy renders enhanced resolution of PET images. While other more specific tracers like Copper are also being studied, the half-life is comparatively short and background signal also prohibitive in some cases. ^{89}Zr-labelled T cells have been successfully employed in clinical

settings to image CAR-T cell trafficking to non-small cell lung cancer (NSCLC), prostate cancer, melanoma, and advanced gastrointestinal malignancies as detailed in **Table 2.**[27,32-34] While the alternative of MRI using superparamagnetic iron oxide nanoparticles that are ingested by cells intended for tracking, this is much more cumbersome and lengthy image acquisition process that is also highly dependent upon cell function rather than precise labeling as would be required for comprehensive imaging of viroimmunotherapy.

The authors propose that an ideal strategy toward comprehensively imaging responses to oncolytic viroimmunotherapy would take into account the "big picture" of a tumor transformation following viral infection, including: 1) immediate changes to cancer cells upon viral entry and replication, 2) initial changes to surrounding tumor immune microenvironment, and 3) finally alterations in tumor immune cell infiltration (**Figure 5a**). Each of these three components of virally-mediated tumor transformation is imageable by tracking virus to tumor with reporter genes, then flagging upregulation of immune checkpoints, and monitoring effector immune cell traffic in treated tumors (**Figure 5b**). In so-doing, investigators would be able to amend treatment courses in real-time to optimize anti-tumor immune responses and prolong patient survival.

CONCLUSION

Herein, we have reviewed the published clinical experience with functional viral imaging and demonstrate additional possible future directions for tracking viral replication in clinical studies. We further reviewed current progress and challenges as well as strategies for future comprehensive imaging of immune responses to oncolytic viral treatment. In conclusion, this

paper emphasizes the importance of continued optimization of preclinical and clinical protocols to visualize viral replication in real-time. While many trials are currently testing imaging endpoints, we must incentivize further investigations to both speed regulatory approvals and incorporate viroimmunotherapy into treatment algorithms. In this era of pay-to-play immunotherapy, patients, clinicians, and payers alike should place high value on real-time proof of viral tumor tropism and therapeutic benefit. Strategies to non-invasively and reliably image viral delivery, checkpoint expression, and immune cell trafficking will be critical to advancement of the field.

MATERIALS AND METHODS

Literature review

PubMed and ClinicalTrials.gov were queried for search terms including but not limited to oncolytic virus, SPECT, PET, imaging, NIS, GFP, optical imaging, functional imaging, tracking. All active clinical trials involving oncolytic viral imaging were reviewed. Trial vectors and key words were used in PubMed to search for any publications of results. Many trials are still accruing.[9,35] Identified publications were included in Table 1 only if a clinically-generated picture was a figure in the manuscript. There were many published abstracts without pictures available, and we anticipate images will be forthcoming from several groups in the near future.

Virus chimerization and hNIS or Fluc cloning

The chimerization, cloning, competitive selection, and sequence of CF33 backbone virus have been described previously.[36-39] Insertion of the hNIS expression cassette or firefly luciferase under the control of the vaccinia H5 promoter or synthetic early (SE) promoter at the *J2R* locus

has also been described,[17,40] as has the deletion of the *F14.5L* gene,[37] and insertion of the anti-PD-L1 transgene at the *F14.5L* locus.[41]

In vitro luciferase activity was confirmed by infecting HCT-116 cells with CF33-Fluc at varying multiplicities of infection (MOIs). Rapid luciferase activity was observed after 24-hours by adding 100x luciferin solution (prepared as below) directly to wells and imaging after 10 minutes with Lago X optical imaging system (Spectral Instruments Imaging, Tucson, AZ).

Cell lines

HT-29 (RRID:CVCL_0320), HCT116 (RRID:CVCL_0291) and African green monkey kidney fibroblasts - CV-1 (RRID:CVCL_0229) cell lines were purchased from ATCC (Manassas, Virginia). All Human colorectal cell lines were maintained in McCoy's 5A medium (Gibco, Gaithersburg, MD) and CV-1 cells were maintained in Dulbecco's modified Eagle's medium (Corning, Corning, NY). MC38 and MC38-Luc cells were a kind gift from Dr. Laleh Melstrom's laboratory (City of Hope, Duarte, CA). MC38 and MC38-Luc cells were maintained in DMEM. All cells were supplemented with 10% fetal bovine serum (FBS) and 1% antibiotic-antimycotic solution, both purchased from Corning (Corning, NY). The cells were maintained in a humidified incubator at 37°C and 5% CO_2. Efforts were made not to perform experiments past 15 passages of cells. All cell lines were tested for mycoplasma before each experiment initiation.

PET imaging

In vivo I-124 uptake measured by PET/CT

Mice bearing HT-29 flank xenografts were divided into imaging and control groups (n=4 mice). To analyze tumor imageability after intratumoral delivery, mice received an intratumoral

injection of 10^4 pfu per tumor of either CF33-hNIS, CF33-Fluc or PBS when tumors reached $100mm^3$. At 7, 14, and 21 days post-viral injection, mice in each group received 200uCi of I-124 injected per tail vein. The radioisotope was obtained from the City of Hope Small Animal Imaging Core Radiopharmacy. PET imaging was then obtained 2 hours following injection using the small animal PET scanner (microPET R4, Siemens Corporation) which provides fully 3-dimensional PET imaging with a spatial resolution of better than 2.0 mm and quantitative accuracy for measurement of tissue activity concentration on the order of 10%. Quantitative accuracy is supported by scatter, dead time and measured attenuation corrections. The system includes a fully developed image analysis package that supports volumetric regions of interest and the fusion of PET with co-registered anatomic CT. To protect mouse thyroids from radioiodine ablation, all mice received T4 supplementation with 5mg levothyroxine/L of water beginning one week before radioiodine administration.

Luciferase imaging

Firefly luciferin solution was prepared as per manufacturer's instruction (PerkinElmer, Waltham, MA). Imaging was obtained after intraperitoneal delivery of luciferin in a control mouse and all mice treated with CF33-Fluc using Lago X optical imaging system (Spectral Instruments Imaging, Tucson, AZ) after 15 minutes incubation.

Tumor models and virus dosing

For the HCT116 xenograft model, 2-3 x 10^6 of HTCT116 cells were injected into 6-8 week old female nude mouse flank using a total of 100 µL PBS containing 50% matrigel for each tumor. When the average tumor size approached 150 mm^3, mice were divided into experimental groups and treated with 10^5 pfu of CF33-Fluc in 50 µL PBS by intravenous or intraperitoneal injection.

Flank tumors of MC38 and MC38-Luc were established using 3-5 x 10^5 cells in matrigel. Tumor measurements and mouse weight were monitored twice weekly using calipers to calculate tumor volume, V (mm^3) = (1/2) x A^2 x B, where A is the shortest, and B is the longest measurement. Treatment typically occurred when tumors reached 100 - 200 mm^3 (approximately 10 days post-cell-injection) following which mice were randomized into treatment groups (n = 4) such that average tumor volume in each group is similar. C57Bl/6J mice aged 8-12 weeks old were used for most experiments (Jackson Laboratories, Bar Harbor, ME & Charles River, Wilmington, MA, RRID:IMSR_JAX:000664, RRID:IMSR_CRL:027). Six-week-old Hsd:Athymic Nude-Foxn1nu female mice (Envigo, Indianapolis, IN) were purchased and acclimatized for seven days.

Mice were maintained in a biosafety containment level 2 facility within our vivarium where the environment was temperature and light controlled with 12-hour light and 12-hour dark cycles, and food and water were ingested *ad libitum*. All animal experiments were performed with approval of the City of Hope Institutional Animal Care and Use Committee (IACUC).

Immunohistochemistry

Tumors were harvested and fixed with 10% formalin. Paraffin-embedded 5 µm thick tumor sections were obtained. The slides were deparaffinized followed by heat-mediated antigen-retrieval per manufacturer's protocol (IHC World, Ellicott City, MD). Tumor slides were then permeabilized with cold methanol and blocked for 30 minutes with TNB Blocking buffer (PerkinElmer, Waltham, MA). Tumor slides were incubated with a rabbit anti-vaccinia virus antibody (Abcam, Cambridge, MA, RRID:AB_778768) 1:100 in TNB blocking buffer in a humidified chamber at 4°C for overnight. The next day, tumor slides were stained with Alexa

Fluor-488-conjugated goat anti-rabbit (Abcam, Cambridge, MA, RRID:AB_2630356) 1:200 in TNB blocking buffer for 1 hour at room temperature. Finally, the slides were counterstained with 4′6-diamidino-2-phenylindole (DAPI). IHC for CD8 was performed by the Pathology Core at City of Hope. Images were obtained using the Nanozoomer 2.0HT digital slide scanner (Hamamatsu Photonics, Hamamatsu City, Shizuoka Pref., Japan) or Ventana iScan HT (Roche, Basel, Switzerland).

Flow cytometry

Single cells from tumors were generated using mouse Tumor Dissociation Kit utilizing GentleMACS dissociator (Miltenyi Biotec, Cologne, Germany). Cells were stained with LIVE/DEAD Fixable dye (Invitrogen, Carlsbad, CA) in PBS for 30 minutes at 4°C in dark. Next, Fc receptors on the cells were blocked using an anti-CD16/32 antibody (BD Biosciences, Franklin Lakes, NJ, RRID: AB_394657 in FACS buffer (PBS containing 2% FBS) for 10 minutes and then stained for 30 minutes at 4°C in the dark using the following antibodies: mouse CD45- peridinin chlorophyll protein complex (PerCP) (Biolegend, San Diego, RRID:AB_893340), mouse CD3- fluorescein isothiocyanate (FITC) (eBiosciences, San Diego, CA, RRID:AB_2572431), mouse CD4-APC (Biolegend, San Diego, CA, RRID:AB_389325) and mouse CD8- VioGreen (Miltenyi Biotec, Cologne, Germany RRID:AB_2659495). The data were acquired using the MACSQuant Analyzer 10 (Miltenyi Biotec, Cologne, Germany). Data were analyzed using the FlowJo software (v10, TreeStar, Ashland, OR).

Statistical Analysis

Statistical analysis was performed using GraphPad Prism (Version 7.01, La Jolla, CA). Student's t-test were used to evaluate statistical significance. $p < 0.05$ was considered significant. Where present in figures, error bars indicate SD or SEM as defined in legends.

AUTHOR CONTRIBUTIONS

Study concept and design: SC, SIK, MO, YF, YW, AP

Data collection, analysis, and interpretation: SC, SIK, MO, JL, SK, ZZ, AY, YF, SGW

Manuscript preparation and critical revision: All authors

Final approval of manuscript: All authors

ACKNOWLEDGMENTS

Funding sources: This work was supported by the American Cancer Society Mentored Research Scholar Grant: MRSG-16-047-01-MPC. Drs. Chaurasiya and Warner are supported by the generosity of the Natalie and David Roberts Family.

Conflicts of Interest: Yuman Fong receives royalties from Merck and from Imugene. CF33 platform is licensed to Imugene by City of Hope. The remaining authors are City of Hope employees but declare no further conflict of interest.

The authors wish to acknowledge Dr. Supriya Deshpande for her expert editorial assistance. This work was completed using the Beckman Research Institute shared facilities that are supported in part by the National Cancer Institute of the National Institutes of Health, grant award P30CA033572. Shyambabu Chaurasiya and Susanne G. Warner wish to thank The Natalie and David Roberts Family for their philanthropy.

342 **Figures** were created using biorender. https://biorender.com

343

REFERENCES

1. Andtbacka RH, Agarwala SS, Ollila DW, Hallmeyer S, Milhem M, Amatruda T, Nemunaitis JJ, Harrington KJ, Chen L, Shilkrut M, et al. Cutaneous head and neck melanoma in OPTiM, a randomized phase 3 trial of talimogene laherparepvec versus granulocyte-macrophage colony-stimulating factor for the treatment of unresected stage IIIB/IIIC/IV melanoma. *Head & neck.* 2016;38(12):1752-1758.
2. Andtbacka RH, Kaufman HL, Collichio F, Amatruda T, Senzer N, Chesney J, Delman KA, Spitler LE, Puzanov I, Agarwala SS, et al. Talimogene Laherparepvec Improves Durable Response Rate in Patients With Advanced Melanoma. *Journal of clinical oncology : official journal of the American Society of Clinical Oncology.* 2015;33(25):2780-2788.
3. Andtbacka RH, Ross M, Puzanov I, Milhem M, Collichio F, Delman KA, Amatruda T, Zager JS, Cranmer L, Hsueh E, et al. Patterns of Clinical Response with Talimogene Laherparepvec (T-VEC) in Patients with Melanoma Treated in the OPTiM Phase III Clinical Trial. *Annals of surgical oncology.* 2016;23(13):4169-4177.
4. Harrington KJ, Andtbacka RH, Collichio F, Downey G, Chen L, Szabo Z, Kaufman HL. Efficacy and safety of talimogene laherparepvec versus granulocyte-macrophage colony-stimulating factor in patients with stage IIIB/C and IVM1a melanoma: subanalysis of the Phase III OPTiM trial. *OncoTargets and therapy.* 2016;9:7081-7093.
5. Ma Y, Wang Q, Dong Q, Zhan L, Zhang J. How to differentiate pseudoprogression from true progression in cancer patients treated with immunotherapy. *American journal of cancer research.* 2019;9(8):1546-1553.
6. Serganova I, Blasberg RG. Molecular Imaging with Reporter Genes: Has Its Promise Been Delivered? *Journal of nuclear medicine : official publication, Society of Nuclear Medicine.* 2019;60(12):1665-1681.
7. Zheng M, Huang J, Tong A, Yang H. Oncolytic Viruses for Cancer Therapy: Barriers and Recent Advances. *Molecular therapy oncolytics.* 2019;15:234-247.
8. Mell LK, Brumund KT, Daniels GA, Advani SJ, Zakeri K, Wright ME, Onyeama SJ, Weisman RA, Sanghvi PR, Martin PJ, et al. Phase I Trial of Intravenous Oncolytic Vaccinia Virus (GL-ONC1) with Cisplatin and Radiotherapy in Patients with Locoregionally Advanced Head and Neck Carcinoma. *Clinical cancer research : an official journal of the American Association for Cancer Research.* 2017;23(19):5696-5702.
9. Wu ZJ, Tang FR, Ma ZW, Peng XC, Xiang Y, Zhang Y, Kang J, Ji J, Liu XQ, Wang XW, et al. Oncolytic Viruses for Tumor Precision Imaging and Radiotherapy. *Human gene therapy.* 2018;29(2):204-222.
10. Dispenzieri A, Tong C, LaPlant B, Lacy MQ, Laumann K, Dingli D, Zhou Y, Federspiel MJ, Gertz MA, Hayman S, et al. Phase I trial of systemic administration of Edmonston strain of measles virus genetically engineered to express the sodium iodide symporter in patients with recurrent or refractory multiple myeloma. *Leukemia.* 2017;31(12):2791-2798.
11. Galanis E, Atherton PJ, Maurer MJ, Knutson KL, Dowdy SC, Cliby WA, Haluska P, Jr., Long HJ, Oberg A, Aderca I, et al. Oncolytic measles virus expressing the sodium iodide symporter to treat drug-resistant ovarian cancer. *Cancer research.* 2015;75(1):22-30.

12. Russell SJ, Federspiel MJ, Peng KW, Tong C, Dingli D, Morice WG, Lowe V, O'Connor MK, Kyle RA, Leung N, et al. Remission of disseminated cancer after systemic oncolytic virotherapy. *Mayo Clinic proceedings.* 2014;89(7):926-933.
13. Barton KN, Stricker H, Brown SL, Elshaikh M, Aref I, Lu M, Pegg J, Zhang Y, Karvelis KC, Siddiqui F, et al. Phase I study of noninvasive imaging of adenovirus-mediated gene expression in the human prostate. *Molecular therapy : the journal of the American Society of Gene Therapy.* 2008;16(10):1761-1769.
14. Penuelas I, Mazzolini G, Boan JF, Sangro B, Marti-Climent J, Ruiz M, Ruiz J, Satyamurthy N, Qian C, Barrio JR, et al. Positron emission tomography imaging of adenoviral-mediated transgene expression in liver cancer patients. *Gastroenterology.* 2005;128(7):1787-1795.
15. Jacobs A, Voges J, Reszka R, Lercher M, Gossmann A, Kracht L, Kaestle C, Wagner R, Wienhard K, Heiss WD. Positron-emission tomography of vector-mediated gene expression in gene therapy for gliomas. *Lancet.* 2001;358(9283):727-729.
16. O'Leary MP, Warner SG, Kim SI, Chaurasiya S, Lu J, Choi AH, Park AK, Woo Y, Fong Y, Chen NG. A Novel Oncolytic Chimeric Orthopoxvirus Encoding Luciferase Enables Real-Time View of Colorectal Cancer Cell Infection. *Molecular therapy oncolytics.* 2018;9:13-21.
17. Warner SG, Kim SI, Chaurasiya S, O'Leary MP, Lu J, Sivanandam V, Woo Y, Chen NG, Fong Y. A Novel Chimeric Poxvirus Encoding hNIS Is Tumor-Tropic, Imageable, and Synergistic with Radioiodine to Sustain Colon Cancer Regression. *Molecular therapy oncolytics.* 2019;13:82-92.
18. Suksanpaisan L, Pham L, McIvor S, Russell SJ, Peng KW. Oral contrast enhances the resolution of in-life NIS reporter gene imaging. *Cancer gene therapy.* 2013;20(11):638-641.
19. Jiang H, DeGrado TR. [(18)F]Tetrafluoroborate ([(18)F]TFB) and its analogs for PET imaging of the sodium/iodide symporter. *Theranostics.* 2018;8(14):3918-3931.
20. Rajecki M, Kangasmaki A, Laasonen L, Escutenaire S, Hakkarainen T, Haukka J, Ristimaki A, Kairemo K, Kangasniemi L, Kiljunen T, et al. Sodium iodide symporter SPECT imaging of a patient treated with oncolytic adenovirus Ad5/3-Delta24-hNIS. *Molecular therapy : the journal of the American Society of Gene Therapy.* 2011;19(4):629-631.
21. Kim S, Park A.K., Chaurasiya, S., Kang, S., Lu, J., Yang, A., Sivanandam, V., Zhang, Z., Woo, Y., Priceman, S.J., Fong, Y., Warner, S.G. Recombinant orthopoxvirus primes colon cancer for checkpoint inhibitor and cross-primes T cells for anti-tumor and anti-viral immunity. *Molecular cancer therapeutics.* 2020.
22. Sampath P, Li J, Hou W, Chen H, Bartlett DL, Thorne SH. Crosstalk between immune cell and oncolytic vaccinia therapy enhances tumor trafficking and antitumor effects. *Molecular therapy : the journal of the American Society of Gene Therapy.* 2013;21(3):620-628.
23. Kim SI, Park AK, Chaurasiya S, Kang S, Lu J, Yang A, Sivanandam V, Zhang Z, Woo Y, Priceman SJ, et al. Recombinant Orthopoxvirus Primes Colon Cancer for Checkpoint Inhibitor and Cross-Primes T Cells for Antitumor and Antiviral Immunity. *Molecular cancer therapeutics.* 2021;20(1):173-182.

24. Liu Z, Ravindranathan R, Kalinski P, Guo ZS, Bartlett DL. Rational combination of oncolytic vaccinia virus and PD-L1 blockade works synergistically to enhance therapeutic efficacy. *Nature communications.* 2017;8:14754.
25. Ribas A, Dummer R, Puzanov I, VanderWalde A, Andtbacka RHI, Michielin O, Olszanski AJ, Malvehy J, Cebon J, Fernandez E, et al. Oncolytic Virotherapy Promotes Intratumoral T Cell Infiltration and Improves Anti-PD-1 Immunotherapy. *Cell.* 2017;170(6):1109-1119 e1110.
26. Gujar S, Pol JG, Kroemer G. Heating it up: Oncolytic viruses make tumors 'hot' and suitable for checkpoint blockade immunotherapies. *OncoImmunology.* 2018:e1442169.
27. Postow MA, Harding JJ, Hellmann MD, Gordon MS, Tsai F, Donoghue JAO, Lewis JS, Wu AM, Le W, Korn RL, et al. Imaging of tumor infiltrating T cells with an anti-CD8 minibody (Mb) 89Zr-IAB22M2C, in advanced solid tumors. 2018;36(15_suppl):e24160-e24160.
28. Weibel S, Basse-Luesebrink TC, Hess M, Hofmann E, Seubert C, Langbein-Laugwitz J, Gentschev I, Sturm VJF, Ye YX, Kampf T, et al. Imaging of Intratumoral Inflammation during Oncolytic Virotherapy of Tumors by F-19-Magnetic Resonance Imaging (MRI). *PloS one.* 2013;8(2).
29. McCarthy CE, White JM, Viola NT, Gibson HM. In vivo Imaging Technologies to Monitor the Immune System. *Frontiers in immunology.* 2020;11:1067.
30. Kurebayashi Y, Choyke PL, Sato N. Imaging of cell-based therapy using (89)Zr-oxine ex vivo cell labeling for positron emission tomography. *Nanotheranostics.* 2021;5(1):27-35.
31. Stojanov K, de Vries EF, Hoekstra D, van Waarde A, Dierckx RA, Zuhorn IS. [18F]FDG labeling of neural stem cells for in vivo cell tracking with positron emission tomography: inhibition of tracer release by phloretin. *Molecular imaging.* 2012;11(1):1-12.
32. Pandit-Taskar N, O'Donoghue JA, Ruan S, Lyashchenko SK, Carrasquillo JA, Heller G, Martinez DF, Cheal SM, Lewis JS, Fleisher M, et al. First-in-Human Imaging with 89Zr-Df-IAB2M Anti-PSMA Minibody in Patients with Metastatic Prostate Cancer: Pharmacokinetics, Biodistribution, Dosimetry, and Lesion Uptake. *Journal of nuclear medicine : official publication, Society of Nuclear Medicine.* 2016;57(12):1858-1864.
33. Niemeijer AN, Leung D, Huisman MC, Bahce I, Hoekstra OS, van Dongen GAMS, Boellaard R, Du S, Hayes W, Smith R, et al. Whole body PD-1 and PD-L1 positron emission tomography in patients with non-small-cell lung cancer. *Nature communications.* 2018;9(1):4664.
34. Moek KL, Waaijer SJH, Kok IC, Suurs FV, Brouwers AH, Menke-van der Houven van Oordt CW, Wind TT, Gietema JA, Schröder CP, Mahesh SVK, et al. ⁸⁹Zr-labeled Bispecific T-cell Engager AMG 211 PET Shows AMG 211 Accumulation in CD3-rich Tissues and Clear, Heterogeneous Tumor Uptake. 2019;25(12):3517-3527.
35. Miller A, Russell SJ. The use of the NIS reporter gene for optimizing oncolytic virotherapy. *Expert opinion on biological therapy.* 2016;16(1):15-32.
36. Chaurasiya S, Chen NG, Lu J, Martin N, Shen Y, Kim SI, Warner SG, Woo Y, Fong Y. A chimeric poxvirus with J2R (thymidine kinase) deletion shows safety and anti-tumor activity in lung cancer models. *Cancer gene therapy.* 2019.
37. Chaurasiya S, Yang A, Kang S, Lu J, Kim SI, Park AK, Sivanandam V, Zhang Z, Woo Y, Warner SG, et al. Oncolytic poxvirus CF33-hNIS-DeltaF14.5 favorably modulates tumor immune microenvironment and works synergistically with anti-PD-L1 antibody in a triple-negative breast cancer model. *Oncoimmunology.* 2020;9(1):1729300.

38. O'Leary MP, Choi AH, Kim SI, Chaurasiya S, Lu J, Park AK, Woo Y, Warner SG, Fong Y, Chen NG. Novel oncolytic chimeric orthopoxvirus causes regression of pancreatic cancer xenografts and exhibits abscopal effect at a single low dose. *Journal of translational medicine.* 2018;16(1):110.
39. Sherman MH, Yu RT, Engle DD, Ding N, Atkins AR, Tiriac H, Collisson EA, Connor F, Van Dyke T, Kozlov S, et al. Vitamin D receptor-mediated stromal reprogramming suppresses pancreatitis and enhances pancreatic cancer therapy. *Cell.* 2014;159(1):80-93.
40. O'Leary MP, Warner SG, Kim S-I, Chaurasiya S, Lu J, Choi AH, Park AK, Woo Y, Fong Y, Chen NG. A Novel Oncolytic Chimeric Orthopoxvirus Encoding Luciferase Enables Real-Time View of Colorectal Cancer Cell Infection. *Molecular Therapy-Oncolytics.* 2018;9:13-21.
41. Woo Y, Zhang Z, Yang A, Chaurasiya S, Park AK, Lu J, Kim SI, Warner SG, Von Hoff D, Fong Y. Novel Chimeric Immuno-Oncolytic Virus CF33-hNIS-antiPDL1 for the Treatment of Pancreatic Cancer. *J Am Coll Surg.* 2020.

493 **Table 1**

Year, *Journal* Author	Virus	Dose (route)	#images per #pts in trial	Disease treated	Actual image	Trial ID
2001 *Lancet* Jacobs et al.	HSV-1-*tk* in liposomal vector DAC-30	Unclear pfu in 30mL (IT)	1/5	Recurrent Glioblastoma	[^{124}I]-FIAU-PET MET-PET FDG-PET MRI brain	None listed
2005 *Gastroenterology* Penuelas et al.	AdCMVtk	2e10-2e12 (IT)	4/7 High dose only	Hepatocellular Carcinoma	PET-CT MRI [^{18}F]FHBG-PET torso	None listed
2008 *Molecular Therapy* Barton K et al.	Ad5-yCD*ut*TK$_{SR39}$ *rep*-hNIS	1e11-1e12 (IPR)	7/12	Prostate cancer	SPECT/CT of multiple pts pelvis	NCT 00583492
2014 *Mayo Clinic Proceedings* Russell S et al.	MV-NIS	1e6-1e11 (IV)	2/2	Recurrent plasma cell myeloma	PET/CT of forehead SPECT/CT & PET of whole body day 1, 8, 15, 28	NCT 00450814
2015 *Cancer Res* Galanis E et al.	MV-NIS	1e8-1e9 (IP)	3/16 High dose only	Drug-resistant ovarian cancer	SPECT/CT left pelvis tumor	NCT 00408590
2017 *Clin Canc Res* Mell et al.	GL-ONC1	3e8 – 3e9 (IV)	#images not reported/ 19	Locoregionally advanced head & neck carcinoma	Fluorescent image of pox lesions noting systemic infection	NCT 01584284
2017 *Leukemia* Dispenzieri A et al.	MV-NIS	1e6-1e11 (IV)	8/32	Refractory Multiple Myeloma	SPECT/CT of legs with light-up on day 7 post-treatment	NCT 00450814

494

495 **Table 2**

Year, *Journal* Author	Image modality	What labelled	#pts imaged	Disease process	Trial ID
2016, *J Nucl Med* Pandit-Taskar N et al.	PET & SPECT	^{89}Zr-Df-IAB2M	18	Prostate Cancer	NCT02760199
2017, *Nature Communications* Niemeijer AN et al.	PET-CT	^{89}Zr-nivolumab	13	NSCLC	2015-004760-11 (EU)
2018, *J Clin Oncol Suppl* Postow M et al.	PET-CT	^{89}Zr-IAB22M2C (Anti-CD8)	3	Melanoma HCC NSCLC	NCT03107663

2019, *Clin Cancer Res* Moek K et al.	PET-CT	^{89}Zr-AMG211 (BiTE CEA/CD3)	9	Advanced GI Cancer	NCT02291614
ClinicalTrials.gov	PET-CT	^{89}Zr-Df - IAB22M2C (Anti-CD8)	ongoing	Melanoma, NSCLC, RCC, SCC	NCT03802123

Figure Legends

Figure 1: PET imaging of ^{124}I uptake and bioluminescent luciferase shows CF33-hNIS and CF33-Fluc tumor tropism

Mice bearing bilateral HT29 flank xenografts were injected in the left flank tumor with CF33-hNIS. (A) On day 7 following viral injection, robust uptake is noted in the injected left-side tumor. (B) On day 14, tumor tropism is shown via uptake in the non-injected right-side tumor. Mice bearing bilateral HCT116 flank xenografts were injected IV or IP with CF33-Fluc. (C) Both IV and IP delivery of CF33-Fluc resulted in tumor luminescence.

Figure 2: Virus co-localizes with tumor infiltrating T cells

(A) On day 10 following euthanasia of mice infected with CF33-Fluc, immunofluorescent vaccinia staining and immunohistochemical CD8+ T cell staining shows co-localization of virally infected cells and tumor-infiltrating T cells. Vaccinia average magnification 0.8x, scale bar = 2.5mm; CD8+ magnification 2x, scale bar = 1mm. (B) Treatment schema (C) Confirmatory experiments using flow cytometry of tumor lysates showed increased CD8+ T cell infiltration as early as 5 days following viral injection. N = 4 per group, stat = unpaired t-test with Welch's correction, ***$p < 0.001$, **$p < 0.01$

Figure 3: In vivo labelling of virally-induced immune checkpoint upregulation

Figure 4: Ex vivo radio-labelling of T cells for image trafficking

Figure 5: Virus-induced tumor changes resulting strategies for comprehensive imaging. (A) schematic showing a "cold" tumor devoid of effector immune cells infected with oncolytic virus, expressing functional reporter protein like hNIS, upregulating immune checkpoint expression, and recruiting and activating immune cells. (B) Opportunities for radiolabeling each step of viral immunogenicity from hNIS expression resulting in radioisotope uptake to anti-body tagging of immune checkpoints to infusing radiolabeled immune cells and examining their traffic to tumors

eTOC

Herein, we review published clinical images of oncolytic viral replication. We examine progress and challenges for future comprehensive imaging of immune responses to oncolytic viral treatment, and propose strategies to non-invasively and reliably image viral delivery, checkpoint expression, and immune cell trafficking.

A

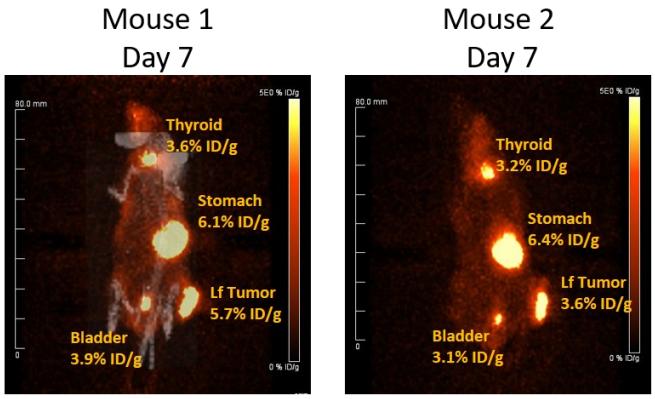

B

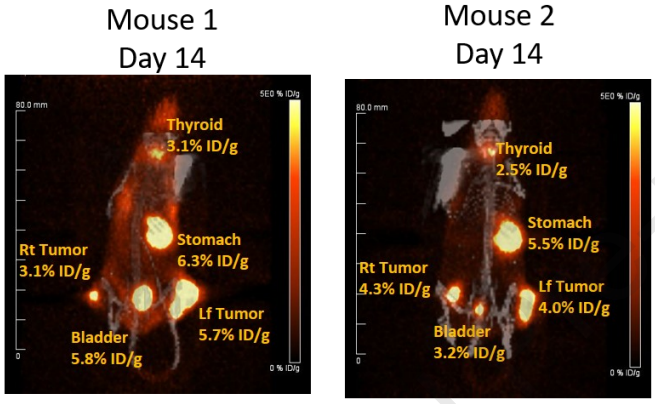

C

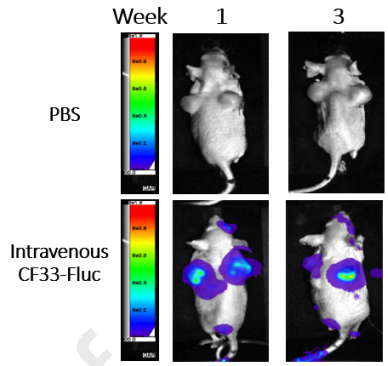

D